Uzbek Mathematical Journal
2026, Volume 70, Issue 1, pp. 165–173
DOI: 10.29229/uzmj.2026-1-18

Thermodynamic analysis of the three-state SOS model on the binary tree

Rahmatullaev M., Karshiboev O.

Abstract. In this work, we investigate the thermodynamic properties of the three-state solid-on-solid (SOS) model on a binary Cayley tree. Employing recurrence relations, we analyze the partition function and derive explicit expressions for the local magnetization and the quadrupolar moment. One of the main results of the paper is the demonstration of the existence of a second-order phase transition in the model. To explore the system's dynamical behavior, we compute the Lyapunov exponent, which reveals transitions between distinct dynamical regimes. Our findings demonstrate the model's rich phase structure, characterized by the emergence of periodic regimes and the absence of chaos, as confirmed by Lyapunov analysis.

Keywords: SOS model, Second-order phase transition, Magnetization, Quadrupolar moment, Lyapunov exponent
MSC (2020): Primary 82B05 · 82B20; Secondary 60K35

1. Introduction

The solid-on-solid (SOS) model is a fundamental framework in statistical mechanics, extensively employed to investigate surface growth, interface dynamics, and phase transitions in lattice systems [1, 2, 3, 4, 5, 6]. By focusing on the height differences between neighboring sites, the SOS model simplifies complex interactions while preserving essential physical phenomena, rendering it a powerful tool for both theoretical and computational studies.

In this work, we examine the three-state SOS model on a Cayley tree of order two (also referred to as a binary tree), which introduces a hierarchical lattice structure that accentuates the role of recursive interactions [3]. The three-state SOS model, in which each site assumes one of three discrete height values, serves as a rich platform for studying phase transitions driven by temperature and coupling strength. Prior investigations of related models have revealed the existence of multiple phases which confirms the existence of the first-order phase transition and critical phenomena in tree-like structures [7, 8, 9, 10, 11, 12].

Here, we employ recursive methods to derive key thermodynamic quantities such as the partition function and magnetization, leveraging the symmetry of the Cayley tree to facilitate analytical progress. We show that the model exhibits the second-order phase transition using stability analysis of fixed points. In addition, we investigate the model's dynamical behavior via the Lyapunov exponent, providing insight into the transition between periodic and chaotic regimes in the recursive dynamics. Our analysis integrates classical methods from statistical physics while offering novel insights into the interplay between thermal and dynamical properties in hierarchical systems. These results contribute to the broader understanding of disordered systems and phase transitions in non-standard geometries.

The structure of the paper is as follows. In Section 2, we define the three-state SOS model on a Cayley tree of order two and derive a system of recurrence relations for the partition function. Section 3 focuses on the thermodynamic behavior of the model, including explicit expressions for the magnetization and quadrupolar moment associated with each fixed point, showing the presence of the second-order phase transition. In Section 4, we examine the dynamical stability of the system through cobweb diagrams, iterative maps, and Lyapunov exponents to characterize periodic and chaotic behavior. Finally, in Section 5, we summarize the main results.

2. Model definition and recursive formulation

We consider the three-state SOS model on a Cayley tree of order two, also known as a binary tree. A Cayley tree of order two is a connected, acyclic graph in which each vertex is connected to

exactly three neighbors, except for the vertices on the boundary (leaves). The tree can be constructed recursively by starting from a root vertex (referred to as the central site) and attaching two new branches to each non-terminal vertex at each successive level. The number of layers, denoted by n, determines the depth of the tree.

The Hamiltonian of the model is given by

$$H = -J \sum_{\langle i,j \rangle} |s_i - s_j|, \tag{2.1}$$

where each spin variable s_i takes one of three possible values: -1, 0, or 1; J is the coupling constant; and the summation is carried out over all nearest-neighbor pairs $\langle i, j \rangle$.

The partition function of the model is

$$Z \equiv \sum_s \exp\left(-\beta H(s)\right) = \sum_s \exp\left(K \sum_{\langle i,j \rangle} |s_i - s_j|\right), \tag{2.2}$$

and here $\beta = 1/T$ (with T being the temperature) and $K = \beta J$. The summation over s in Eq. (2.2) denotes the sum over all possible spin configurations on the tree.

Phase transitions are fundamental phenomena in statistical physics, often identified through the emergence of multiple Gibbs measures. Following [9], the existence of at least two distinct Gibbs states at a temperature T indicates a first-order phase transition. A second-order phase transition is characterized by the continuous emergence of nonzero spontaneous magnetization from zero as the parameter crosses a critical value, accompanied by a change in stability of the fixed points in the recursive dynamical system.

The model defined by the Hamiltonian (2.1) on a Cayley tree of order two can be studied analytically and numerically using the method of recursion relations. The approach is based on the hierarchical structure of the tree.

Since the analysis focuses on the bulk behavior of the system (i.e., deep inside the Cayley tree), it is important to note that all interior sites are statistically equivalent due to the tree's symmetry [8]. When the Cayley tree is cut at the central site (denoted as site 0; see Fig. 1), it splits into three identical subtrees.

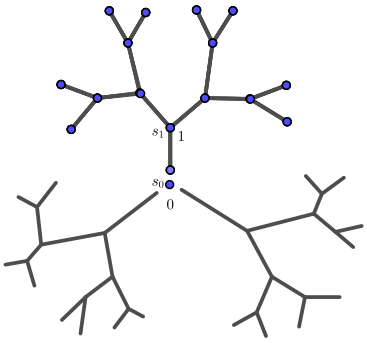

Figure 1. Structure of the Cayley tree of order two rooted at site 0.

This symmetry allows the partition function (2.2) to be rewritten in the simplified form:

$$Z = \sum_{s_0} \left[g_n(s_0)\right]^3, \tag{2.3}$$

where $s_0 \in \{-1, 0, 1\}$, and the functions $g_n(s_0)$ satisfy the recursion relation

$$g_n(s_0) = \sum_{s_1} \exp\left(K|s_0 - s_1|\right) \left[g_{n-1}(s_1)\right]^2. \tag{2.4}$$

Here, $g_n(s_0)$ represents the contribution to the partition function from a subtree of depth n rooted at a site with spin value s_0, and s_1 denotes the spin values at the next layer of the tree. It is assumed that the tree has n layers in total.

It is often more convenient to work with recursion relations defined as ratios of the functions in Eq. (2.4), namely,

$$x_n = \frac{g_n(-1)}{g_n(1)}, \qquad y_n = \frac{g_n(0)}{g_n(1)}. \tag{2.5}$$

The explicit form of the recursion relations for x_n and y_n in Eq. (2.5) is given by

$$\begin{cases} x_n = \dfrac{x_{n-1}^2 + \theta y_{n-1}^2 + \theta^2}{\theta^2 x_{n-1}^2 + \theta y_{n-1}^2 + 1}, \\ \\ y_n = \dfrac{\theta x_{n-1}^2 + y_{n-1}^2 + \theta}{\theta^2 x_{n-1}^2 + \theta y_{n-1}^2 + 1}, \end{cases} \tag{2.6}$$

where $\theta = \exp(K)$. The fixed point values of x_n and y_n in the limit $n \to \infty$ are obtained by solving the steady-state version of Eq. (2.6), which leads to the system:

$$\begin{cases} x = \dfrac{x^2 + \theta y^2 + \theta^2}{\theta^2 x^2 + \theta y^2 + 1}, \\ \\ y = \dfrac{\theta x^2 + y^2 + \theta}{\theta^2 x^2 + \theta y^2 + 1}. \end{cases} \tag{2.7}$$

In [3], the complete solution of the system (2.7) is presented, and the occurrence of a first-order phase transition for the model is established. In the present paper, we further demonstrate that the model also exhibits a second-order phase transition. Moreover, [3] shows that there exist two critical values of θ:

- $\theta_c \approx 0.1414$, which is the solution of the algebraic equation

$$4\theta^7 + 12\theta^5 + 71\theta^4 + 12\theta^3 - 38\theta^2 + 12\theta - 1 = 0,$$

- and $\theta_c' = \frac{1}{3}\left(\sqrt[3]{26+6\sqrt{33}} - \frac{8}{\sqrt[3]{26+6\sqrt{33}}} - 1\right) \approx 0.2956.$

The set of solutions to the system (2.7) is summarized in the following result:

Lemma 2.1 ([3])**.** *The number of fixed points of the system* (2.7) *depends on the value of the parameter* θ *as follows:*

- *If* $\theta > \theta_c'$*, the system has a unique solution* $(x^{(1)}, y^{(1)})$*;*
- *If* $\theta = \theta_c'$*, the system has three solutions:* $(x^{(1)}, y^{(1)})$*,* $(x^{(4)}, y^{(4)})$*, and* $(x^{(6)}, y^{(6)})$*;*
- *If* $\theta_c < \theta < \theta_c'$*, the system has five solutions:* $(x^{(1)}, y^{(1)})$ *and* $(x^{(i)}, y^{(i)})$ *for* $i = 4, 5, 6, 7$*;*
- *If* $\theta = \theta_c$*, the system has six solutions:* $(x^{(1)}, y^{(1)})$ *and* $(x^{(i)}, y^{(i)})$ *for* $i = 3, 4, 5, 6, 7$*;*
- *If* $\theta < \theta_c$*, the system has seven solutions:* $(x^{(i)}, y^{(i)})$ *for* $i = 1, 2, 3, 4, 5, 6, 7$.

Here, the values $y^{(i)}$ *for* $i = 1, 2, 3$ *(ordered as* $y^{(3)} < y^{(2)} < y^{(1)}$*, if they exist) are the roots of the cubic equation*

$$\theta y^3 - y^2 + (\theta^2 + 1)y - 2\theta = 0,$$

which can be solved explicitly using Cardano's formula. For these roots, $x^{(1)} = x^{(2)} = x^{(3)} = 1$*. The remaining* $x^{(i)}$ *and* $y^{(i)}$ *values for* $i = 4, 5, 6, 7$ *are given by:*

$$x^{(4)} = \frac{1}{2}\left(\xi_2 - \sqrt{\xi_2^2 - 4}\right), \quad x^{(5)} = \frac{1}{2}\left(\xi_1 - \sqrt{\xi_1^2 - 4}\right),$$
$$x^{(6)} = \frac{1}{2}\left(\xi_1 + \sqrt{\xi_1^2 - 4}\right), \quad x^{(7)} = \frac{1}{2}\left(\xi_2 + \sqrt{\xi_2^2 - 4}\right),$$

where

$$\xi_1 = \frac{1-3\theta^2-\sqrt{(\theta-1)(\theta^3+\theta^2+3\theta-1)}}{2\theta^2},\ \ \xi_2 \ \ = \frac{1-3\theta^2+\sqrt{(\theta-1)(\theta^3+\theta^2+3\theta-1)}}{2\theta^2},$$

and the corresponding $y^{(i)}$ *values are given by*

$$y^{(i)} = \frac{1}{\sqrt{\theta}}\sqrt{(1-\theta^2)x^{(i)} - \theta^2\left((x^{(i)})^2+1\right)}, \quad i = 4,5,6,7.$$

3. The presence of the second-order phase transition

In this section, we analyze the thermodynamic behavior of the three-state SOS model on the binary Cayley tree using the recursive framework established in the previous section. By utilizing the explicit expressions derived from the recurrence relations, we compute key physical observables such as the local magnetization and the quadrupolar moment. Using these, we show that there is a second-order phase transition.

3.1. **Local Magnetization.** The local magnetization is defined by

$$M = Z^{-1}\sum_{s_0} s_0 \exp\{-\beta H\}, \tag{3.1}$$

where the sum is taken over the possible spin states at the root of the Cayley tree.

Using the representation of the recursion relations given in Eqs. (2.2)–(2.6), the spontaneous magnetization per site is obtained as

$$M = \frac{1-x^3}{x^3+y^3+1}, \tag{3.2}$$

where (x, y) is any solution of the fixed point equations (2.7).

We denote by M_i the magnetization corresponding to the fixed point $(x^{(i)}, y^{(i)})$, $i = 1, \ldots, 7$, i.e.,

$$M_i = \frac{1-(x^{(i)})^3}{(x^{(i)})^3+(y^{(i)})^3+1}, \qquad i = 1,\ldots,7. \tag{3.3}$$

Note that for $i = 1, 2, 3$, we have $x^{(i)} = 1$, hence $M_i = 0$ for these indices. In Fig. 2, plots of magnetizations M_i for $i = 4, 5, 6, 7$ are drawn.

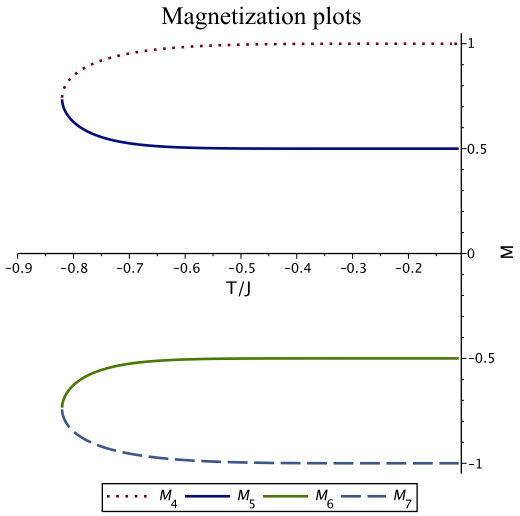

Figure 2. Plots of the magnetizations M_i for $i = 4, \ldots, 7$ are presented. At low temperatures and for $J < 0$, the magnetizations M_4, M_5, M_6, and M_7 take nonzero values with opposite signs. As the temperature increases, their magnitudes gradually decrease and eventually vanish continuously at the critical temperature.

Equation (3.2) shows that the local magnetization has zero value only when $x = 1$. Therefore, the second-order phase transition can be realized at some value of the temperature only for $x = 1$ with a corresponding definite value of y. The model exhibits a second-order phase transition at the critical point θ_c' (≈ 0.2956), where for $\theta < \theta_c'$, there are two stable fixed points with $x \neq 1$, corresponding to nonzero local magnetization.

Now, we show that the system (2.7) has two stable fixed points with $x \neq 1$. Note that the Jacobian at a fixed point (x, y) of (2.7) can be calculated as follows (see [12]):

$$\mathbb{J}(x,y,\theta) = \begin{pmatrix} \frac{-2x(\theta^2-1)(\theta y^2+\theta^2+1)}{(\theta^2x^2+\theta y^2+1)^2} & \frac{2\theta y(\theta^2-1)(x^2-1)}{(\theta^2x^2+\theta y^2+1)^2} \\ \frac{-2x\theta(\theta^2-1)}{(\theta^2x^2+\theta y^2+1)^2} & \frac{-2y\theta(\theta^2-1)}{(\theta^2x^2+\theta y^2+1)^2} \end{pmatrix}. \tag{3.4}$$

We find the eigenvalues of the matrix (3.4):

$$\lambda_\pm(x,y,\theta) = \frac{-B \pm (\theta^2-1)\sqrt{D}}{A},$$

where

$$A = A(x,y,\theta) := \left(\theta^2x^2 + \theta\, y^2 + 1\right)^2,$$

$$B = B(x,y,\theta) := \theta\, xy^2 + \theta^2 x + \theta\, y + x,$$

$$\begin{aligned} D = D(x,y,\theta) :=& \theta^4x^2 + \left(2\,x^2y^2 - 2\,xy\right)\theta^3 + \left(2\,x^2y^2 - 2\,xy\right)\theta + x^2 + \\ &+ \left(x^2y^4 - 2\,xy^3 + y^2 + \left(-4\,x^3 + 4\,x\right)y + 2\,x^2\right)\theta^2 \end{aligned}$$

By Lemma 2.1, it is known that $x^{(i)} \neq 1$, $i = 4, 5, 6, 7$. Note that the functions $\lambda_\pm$ at fixed points depend solely on θ and do not involve any additional parameters. From the graphs (see Figs. 3 and 4), one can observe that

- $|\lambda_\pm(x^{(4)}, y^{(4)}, \theta)| < 1$ for $\theta < \theta_c'$;
- $|\lambda_\pm(x^{(5)}, y^{(5)}, \theta)| < 1$ for $\theta < \theta_c'$;
- $|\lambda_+(x^{(6)}, y^{(6)}, \theta)| < 1$ for $\theta < \theta_c'$ and $|\lambda_-(x^{(6)}, y^{(6)}, \theta)| > 1$ for $\theta < \theta_c'$;
- $|\lambda_+(x^{(7)}, y^{(7)}, \theta)| < 1$ for $\theta < \theta_c'$ and $|\lambda_-(x^{(7)}, y^{(7)}, \theta)| < 1$ for $\theta < \widehat{\theta}$ (≈ 0.2949) and $|\lambda_-(x^{(7)}, y^{(7)}, \theta)| \geq 1$ for $\widehat{\theta} \leq \theta < \theta_c'$.

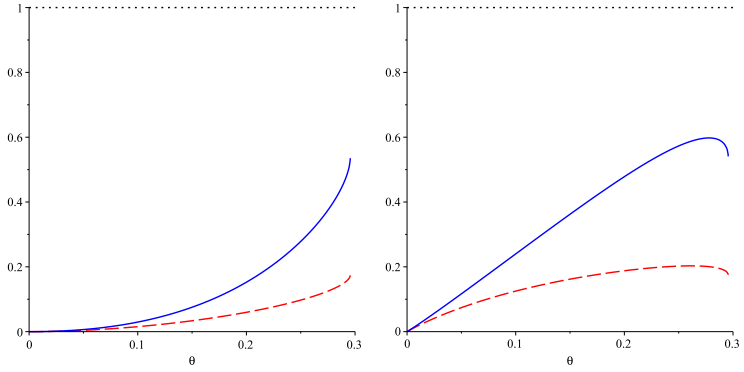

Figure 3. Plots of the functions (left) $|\lambda_\pm(x^{(4)}, y^{(4)}, \theta)|$ for $\theta < \theta_c'$ and (right)$|\lambda_\pm(x^{(5)}, y^{(5)}, \theta)|$ for $\theta < \theta_c'$.

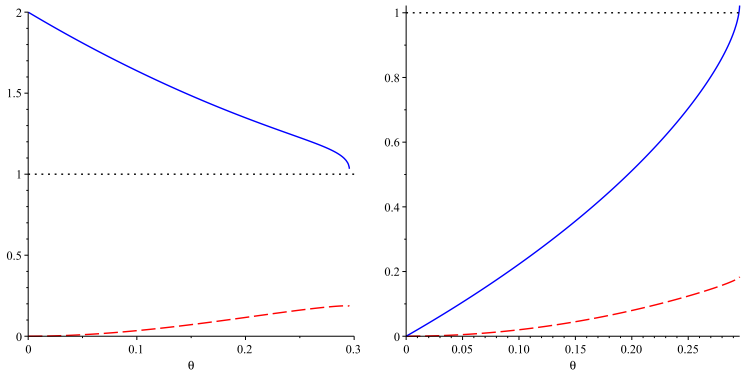

Figure 4. Plots of the functions (left) $\mid \lambda_{\pm}(x^{(6)}, y^{(6)}, \theta) \mid$ for $\theta < \theta_c'$ and (right)$\mid \lambda_{\pm}(x^{(7)}, y^{(7)}, \theta) \mid$ for $\theta < \theta_c'$.

Thus, we conclude that the model exhibits the second-order phase transition.

3.2. **Quadrupolar Moment.** In the subsection, we calculate quadrupolar moment of the model.

The quadrupolar moment is defined by

$$Q = Z^{-1} \sum_{s_0} s_0^2 \exp\{-\beta H\}. \tag{3.5}$$

Using the same recursive framework, the quadrupolar moment is given by

$$Q = \frac{1 + x^3}{x^3 + y^3 + 1}, \tag{3.6}$$

where (x, y) is a fixed point of Eq. (2.7).

Let Q_i denote the quadrupolar moment corresponding to $(x^{(i)}, y^{(i)})$, $i = 1, \ldots, 7$, i.e.,

$$Q_i = \frac{1 + (x^{(i)})^3}{(x^{(i)})^3 + (y^{(i)})^3 + 1}, \qquad i = 1, \ldots, 7. \tag{3.7}$$

One can show that $Q_4 = Q_7$ and $Q_5 = Q_6$ for $\theta \leq \theta_c'$. In Fig 5, plots of quadrupolar moments Q_i for $i = 1, \ldots, 5$ are drawn.

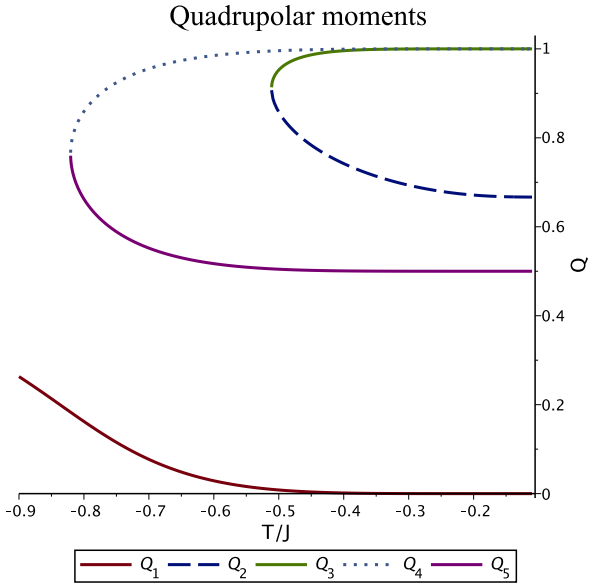

Figure 5. Plots of the quadrupolar moments Q_i for $i = 1, \ldots, 5$ are presented. At low temperatures and for $J < 0$, the quadrupolar moments Q_1, Q_2, Q_3, Q_4, and Q_5 take distinct nonzero values. As the temperature increases, they show a slight decrease.

4. Dynamical analysis

In this section, we investigate the regions where the model exhibits chaotic or periodic behavior. This is achieved through the numerical computation of Lyapunov exponents and visualization of the iteration dynamics via cobweb diagrams.

4.1. **Cobweb Diagrams and Map Iterations.** We begin by analyzing the recurrence equation (2.7) under the simplifying assumption $x = 1$. Under this constraint, the equation reduces to the following rational map:

$$y = f(y) = \frac{y^2 + 2\theta}{\theta y^2 + \theta^2 + 1}. \tag{4.1}$$

The stability of fixed points in such dynamical systems is a key factor in understanding the nature of phase transitions. Cobweb diagrams and iterative maps are classical numerical tools used to study the qualitative behavior of these systems.

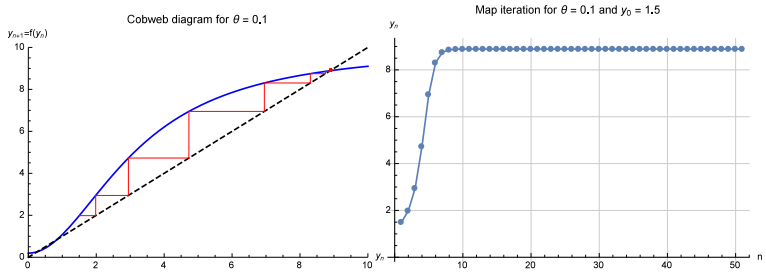

Figure 6. Cobweb diagram and iteration map for the dynamical system (4.1) with parameters $\theta = 0.1$, $y_0 = 1.5$. The system is iterated 50 times. Three distinct fixed points are observed, one of which is repelling.

Figure 6 shows the cobweb and iteration plots generated using *Mathematica* [13] for $\theta = 0.1$ and initial condition $y_0 = 1.5$. The iteration reveals three fixed points, with one repelling and two attracting.

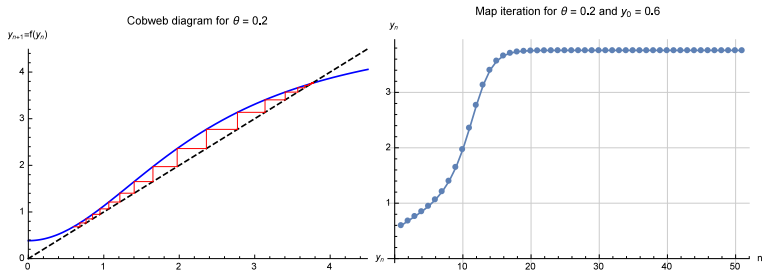

Figure 7. Cobweb diagram and iteration map for the dynamical system (4.1) with parameters $\theta = 0.2$, $y_0 = 0.6$. The system is iterated 50 times. A single attracting fixed point is observed.

In Figure 7, for $\theta = 0.2$ and $y_0 = 0.6$, the system converges to a unique attracting fixed point, highlighting parameter sensitivity in the system's long-term behavior.

4.2. **Lyapunov Exponent.** To further assess the stability and possible chaotic behavior of the system, we compute the Lyapunov exponent. This quantity quantifies the average exponential rate of divergence (or convergence) of nearby trajectories in phase space [14, 15]. For the rational map (4.1),

$$y_n = f(y_{n-1}) = \frac{y_{n-1}^2 + 2\theta}{\theta y_{n-1}^2 + \theta^2 + 1}, \tag{4.2}$$

the Lyapunov exponent is defined as

$$\lambda = \lim_{N\to\infty} \frac{1}{N} \sum_{n=1}^{N} \ln |f'(y_n)|, \tag{4.3}$$

where the derivative of $f(y)$ is given by

$$f'(y) = \frac{2y(1-\theta^2)}{(\theta y^2 + \theta^2 + 1)^2}. \tag{4.4}$$

Thus, the Lyapunov exponent becomes

$$\lambda = \lim_{N\to\infty} \frac{1}{N} \sum_{n=1}^{N} \ln \left| \frac{2(1-\theta^2)y_n}{(\theta y_n^2 + \theta^2 + 1)^2} \right|. \tag{4.5}$$

To numerically compute λ, the map is iterated for different values of θ, with transient dynamics discarded, and the long-term average evaluated. This provides insight into the periodic or chaotic nature of the system.

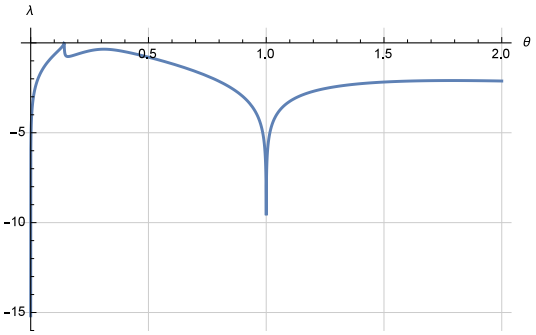

Figure 8. Lyapunov exponent λ of the rational map (4.2) as a function of the parameter θ. Each data point is based on 1000 iterations. The negative values of λ indicate stable periodic behavior.

As seen in Fig. 8, the Lyapunov exponent remains negative across the range of θ, indicating that the system exhibits periodic (non-chaotic) behavior. These findings are consistent with previous studies of lattice models on Cayley trees [16, 17], where the dynamical systems were found to be predominantly regular, with chaotic behavior being rare or absent.

5. Conclusion

In this paper, we analyzed the three-state SOS model on the binary Cayley tree using a recursive approach. Specifically, we studied the temperature dependence of magnetization and quadrupolar moments in the case $J < 0$. Our results show that M_1, M_2, and M_3 remain zero at all temperatures, while nonzero magnetization appears only for M_4, M_5, M_6, and M_7. These exhibit opposite signs at low temperatures, indicating antiferromagnetic order. As temperature increases, the magnetizations decrease and vanish continuously at the critical point, confirming a second-order phase transition.

The quadrupolar moments behave differently: they stay finite at low temperatures, decrease slightly with increasing temperature, but do not vanish at the critical point. This demonstrates that once magnetic order is lost, a nematic (hidden) phase still persists in the system. Hence, for $J < 0$, the three-state SOS model exhibits the following sequence of phases with increasing temperature: antiferromagnetic $\to$ nematic $\to$ paramagnetic.

A dynamical systems analysis further shows that the model's behavior is periodic, with the Lyapunov exponent remaining negative across all values of θ, confirming the absence of chaos.

Acknowledgments. We thank the referees for the careful reading of the manuscript and especially for a number of suggestions that have improved the paper.

References

[1] Jahnel B., Rozikov U., Three-state p-SOS models on binary Cayley trees. J. Stat. Mech. Theory Exp. (2024) Vol. 2024, Iss. 11,

[2] Karshiboev O., Periodic Gibbs measures for the three-state SOS model on a Cayley tree with a translation-invariant external field. Theor. Math. Phys. (2022) Vol. 212, P. 1276–1283.

[3] Kuelske C., Rozikov U., Extremality of translation-invariant phases for a three-state SOS model on the binary tree. J. Stat. Phys. (2015) Vol. 160, P. 659–680.

[4] Rahmatullaev M., Abraev B., Non-translation invariant Gibbs measures of an SOS model on a Cayley tree. Rep. Math. Phys. (2020) Vol. 86, Iss. 3, P. 345–360.

[5] Rahmatullaev M., Karshiboev O., Gibbs measures for the three-state SOS model with external field on a Cayley tree. Positivity, (2022),

[6] Rozikov U., Suhov Y., Gibbs measures for SOS models on a Cayley tree. Inf. Dim. Anal. Quant. Prob. Rel. Fields, (2006),

[7] Rozikov U., Gibbs Measures on Cayley Trees. World Scientific, Singapore, (2013).

[8] Baxter R., Exactly Solved Models in Statistical Mechanics. Academic Press, London/New York, (1982).

[9] Friedli S., Velenik Y., Statistical Mechanics of Lattice Systems: A Concrete Mathematical Introduction. Cambridge University Press, (2017).

[10] Sinai Y., Theory of Phase Transitions: Rigorous Results. Science, Moscow, (1980).

[11] Mukhamedov F., Extremality of disordered phase of λ-model on Cayley tree. Algorithms, (2022) Vol. 15, P. 18.

[12] Rozikov U., An Introduction to Mathematical Billiards. World Scientific, Hackensack, NJ, (2019).

[13] Wolfram Research I., Mathematica, Version 8.0. Wolfram Research, Inc., Champaign, IL, (2010).

[14] Alligood K., Sauer T., Yorke J., Chaos: An Introduction to Dynamical Systems. Springer, (2000).

[15] Devaney R., An Introduction to Chaotic Dynamical Systems. Benjamin-Cummings, Menlo Park, CA, (1986).

[16] Akin H., Calculation of some thermodynamic quantities for the Ising model on a kth order Cayley tree. Physica B, (2023) Vol. 662,

[17] Akin H., On the periodicity of the rational dynamical system corresponding to the Vannimenus-Ising model. J. Comput. Nonlinear Dynam. (2023) Vol. 18, Iss. 1,

Rahmatullaev M.M.,
V.I.Romanovskiy Institute of Mathematics,
Uzbekistan Academy of Sciences,
Tashkent, Uzbekistan
e-mail: mrahmatullaev@rambler.ru

Karshiboev O.Sh.,
Oriental university, Samarkand campus, Uzbekistan
e-mail: okarshiboevsher@mail.ru